THE EFFECT OF PRESSURE ANISOTROPY ON BALLOONING MODES IN TOKAMAK PLASMAS

M. J HOLE, A. JOHNSTON, Z. S. QU, H. HEZAVEH
Mathematical Sciences Institute
Australian National University
Acton 0200 ACT, AUSTRALIA
Email: matthew.hole@anu.edu.au

A. BARNES
School of Physics and Astronomy,
Monash University,
Clayton Victoria 3800, Australia

Abstract

Edge Localised Modes (ELMs) are thought to be caused by a spectrum of magnetohydrodynamic instabilities, including the ballooning mode. While ballooning modes have been studied extensively both theoretically and experimentally, the focus of the vast majority of this research has been on isotropic plasmas. The prevalence of pressure anisotropy in modern tokamaks thus motivates further study of these modes. This paper presents a numerical analysis of ballooning modes in anisotropic equilibria. The investigation was conducted using the newly-developed codes HELENA+ATF and MISHKA-A, which adds anisotropic physics to equilibria and stability analysis. We have examined the impact of anisotropy on the stability of an n=30 ballooning mode, confirming results conform to previous calculations in the isotropic limit. Growth rates of ballooning modes in equilibria with different levels of anisotropy were then calculated using the stability code MISHKA-A. The key finding was that the level of anisotropy had a significant impact on ballooning mode growth rates. For $T_\perp > T_\parallel$, typical of ICRH heating, the growth rate increases, while for $T_\perp < T_\parallel$, typical of neutral beam heating, the growth rate decreases. We also report preliminary studies on equilibrium remapping tools to accommodate an arbitrary level of anisotropy for arbitrary aspect ratio and cross-section. The purpose of these studies is to utilize HELENA+ATF and MISHKA-A to examine the impact of anisotropy on the equilibrium and stability of ITER scenarios, and cross-validate these calculations to experiments.

1. INTRODUCTION

It is well known that neutral beam injection and ion cyclotron resonance heating can induce pressure anisotropy, in which the pressure perpendicular and parallel to the magnetic field lines is different (see for instance the review article and references therein of Hole and Fitzgerald [1]). In JET, ICRH can cause anisotropies of $p_\perp/p_\parallel \sim 2.5$ [2], where $p_\perp$ ($p_\parallel$) refers to the total plasma pressure perpendicular (parallel) to the magnetic field lines. In the UK's Mega Ampere Spherical Tokamak (MAST), parallel NBI heating can lead to anisotropy of up to $p_\parallel / p_\perp \sim 1.7$[3]. Despite the prevalence of anisotropy in modern tokamaks, it remains absent from most MHD treatments.

Recently, Qu *et al* modified the equilibrium and stability codes to capture the effects of pressure anisotropy. These new codes, HELENA+ATF[4] and MISHKA-A[5], permit the numerical study of tokamak instabilities in anisotropic conditions. The code combination has been used to analyse the growth rates of internal n=1 current-driven modes in anisotropic equilibria, and the frequency and mode structure of Alfvénic gap modes.

The investigation of the effects of pressure anisotropy on marginal stability of ballooning modes and interchange modes, both of which can be derived from the ballooning mode equation, (e.g. Pogutse[6], and the book by Goedbloed[7] and references therein) has been investigated by a number of authors. Such work however has focused principally on analytic expressions for marginal stability for n=∞ ballooning modes in very large aspect ratio circular cross section geometry. In this work the impact on growth rate of pressure anisotropy on finite n ballooning modes is examined.

We also report preliminary studies on equilibrium remapping tools to accommodate an arbitrary level of anisotropy for arbitrary aspect ratio and cross-section. The purpose of these studies is to utilize HELENA+ATF and MISHKA-A to examine the impact of anisotropy on the equilibrium and stability of ITER scenarios[8], and cross-validate these calculations to experiments.

2. MODELLING ANISOTROPIC PLASMAS

A stationary, anisotropic plasma can be defined by the following equations:

$$\nabla \cdot \mathbf{B} = 0, \tag{1}$$

$$\nabla \times \mathbf{B} = \mu_0 \mathbf{J}, \tag{2}$$

$$\nabla \cdot \bar{\boldsymbol{P}} = \mathbf{J} \times \mathbf{B}, \tag{3}$$

$$\bar{P} = p_{\perp}\boldsymbol{I} + \frac{\triangle \boldsymbol{BB}}{\mu_0}, \tag{4}$$

$$\Delta = \mu_0 \frac{p_{||} - p_{\perp}}{B^2}, \tag{5}$$

In a tokamak the following steps can be taken to reduce the equations to a single ode for ψ: (1) write the field in Clebsch form with a scalar toroidal field, (2) decompose the current densities into toroidal and poloidal components, (3) write the enthalpy as W(ρ, B, ψ) as a flux function, H(ψ), (4) select a bi-Maxwellian distribution model for the pressures and temperatures,

$$p_{||}(\rho, B, \phi) = \rho T_{||}(\psi), \tag{6}$$

$$p_{\perp}(\rho, B, \phi) = \rho T_{\perp}(B, \psi), \tag{7}$$

(5) rearrange for *W* and $T_{\perp}$,

$$H(\psi) = W(\rho, B, \phi) = T_{||} \ln \frac{T_{||}\rho}{T_{\perp}\rho_0}, \tag{8}$$

$$T_{\perp}(B, \psi) = \frac{T_{||}B}{|B - T_{||}\Theta(\psi)|}, \tag{9}$$

(6) re-arrange Eq. (3) for the pressure gradient,

$$\mu_0 \nabla p_{||} = \frac{\Delta \nabla B^2}{2} + \nabla \times [(1 - \Delta)\mathbf{B}\,] \times \mathbf{B}, \tag{10}$$

and finally (7) consider the component of Eq. (10) in the ∇ψ direction, giving

$$\nabla \cdot \frac{(1-\Delta)\nabla\psi}{R^2} = -\frac{FF'}{(1-\Delta)R^2} - \mu_0 \rho \left[T_{||} + H' - \left(\frac{\partial W}{\partial \psi}\right)_{\rho,B} \right], \tag{11}$$

where $F = RB_{\phi}(1-\nabla)$ is a generalised toroidal flux function. Equation (11) is a generalised Grad-Sharfanov equation for the poloidal flux ψ. It is constrained by four flux functions: {H, $T_{||}$, F, Θ}, as well as the boundary conditions for ψ, as well as the plasma boundary.

The stability codes used in this work are MISHKA[9] and MISHKA-A. Both stability treatments assume zero equilibrium flow, and solve for the linear perturbed magnetic field and fluid velocity using a Fourier expansion with poloidal and toroidal mode numbers *m* and *n* respectively, and radially in cubic/quadratic Hermite elements. The problem is reduced to an eigenvalue problem, and solved for given *n* and a range of *m*.

3. BALLOONING MODES OF A LARGE ASPECT RATIO TOKAMAK

Our starting point is identifying a ballooning mode using the isotropic tool chain of HELENA and MISHKA. We follow Huysmans *et al*[10], who used the equilibrium profiles

$$p'(\psi) = p_0(1 - \psi_n + p_1 \left[(\psi_n - \psi_b)^2(3 - 2\psi_n - \psi_b)/(1 - \psi_b)\right]^{1/4}), \tag{12}$$

$$\langle J \rangle = J_0 \left(1 - 0.8\psi_n - 0.2{\psi_n}^2\right), \tag{13}$$

where ψ_n is a normalised poloidal flux, the parameters p_0, J_0 are the on-axis pressure-gradient and current density, p_1 and ψ_b characterise the pedestal height and position, respectively, and the angled brackets denote flux surface averaging. Following Huysmans *et al*, we set ψ_b=0.9, assume a circular cross-section tokamak, an inverse aspect ratio of R_0/a=4, poloidal beta β_{pol} =1, and edge q_a=4. Like Husyman *et al*, we have studied an *n*=30 ballooning mode. Figure 1 plots the eigenfunction, with poloidal mode number range restricted to 90<*m*<120, such that the mode is resonant with the edge pedestal, where 3<q<4.

At present, MISHKA-A assumes a conformal wall at the plasma boundary. To conduct a meaningful study of stability, we have adapted the previous HELENA equilibrium to include an artificial vacuum. This was achieved by shifting the pressure input profile to HELENA, such that it was equal to zero for ψ_{vac}>0.95, while keeping the current profile and all other parameters the same.

We have modified the equilibrium remapping technique developed by Qu *et al*[5] to explore the impact of anisotropy on the internal kink mode. The remapping approach produces the same q profile and thermal energy $p = (2p_{\perp} + p_{||})/3$ by taking as input an isotropic equilibrium produced using HELENA+ATF, and a value for

parameter $\widetilde{\Theta}_0 = R_0\Theta_0 T_0/F_0 = T_0/T_{||}\left(1 - T_{||}/T_\perp\right)$, where R_0 is the major radius, while T_0 and F_0, respectively, define the values of the temperature and toroidal flux at ψ=0. The anisotropy of the plasma is defined through Eq. (9). In detail, the procedure involves setting $J_{\phi i} = J_{\phi a}$, assuming that $B_\theta/B_\phi \ll 1$ and expanding for small Δ to give $F_a^2 \approx F_i^2(1 - \frac{4}{3}\Delta)$.

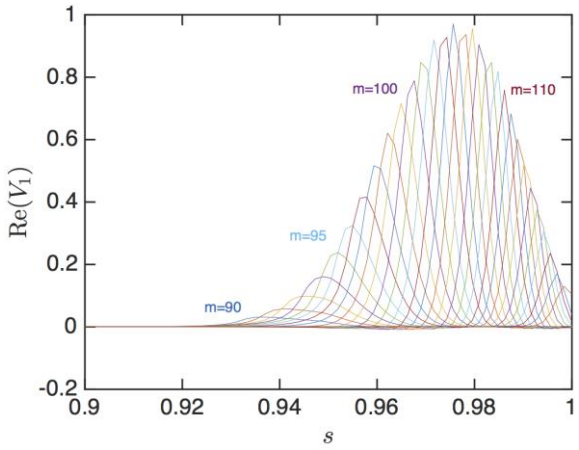

Fig. 1: . Radial mode structure of an n = 30 instability found using MISHKA. The wall is placed at $R_w/a = 2$.

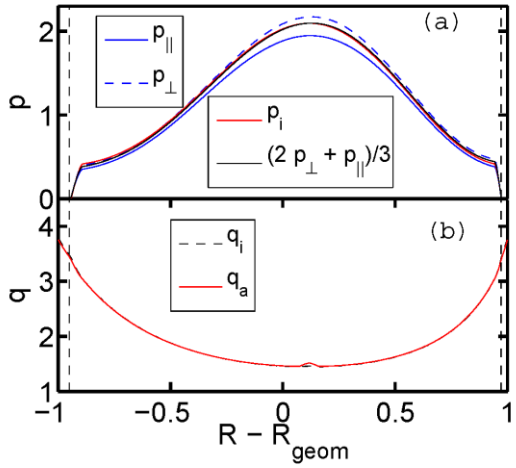

Fig. 2: HELENA+ATF equilibrium for isotropic ($\widetilde{\Theta}_0 = 0.0$) / anisotropic ($\widetilde{\Theta}_0 = 0.1$) plasmas, showing (a) pressure and (b) q profiles. The dashed vertical lines denote the plasma-vacuum boundary, with vacuum for $\psi_n > 0.95$

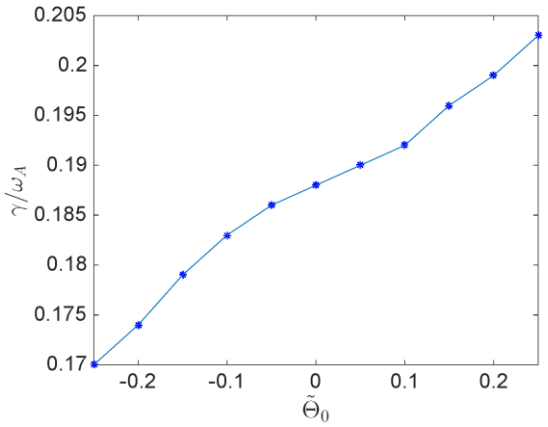

Fig. 3: The relationship between growth rate and $\widetilde{\Theta}_0$ for the n = 30 mode. For $\widetilde{\Theta}_0 > 0$, $T_{||}/T_\perp < 1$, and for $\widetilde{\Theta}_0 < 0$, $T_{||}/T_\perp < 1$.

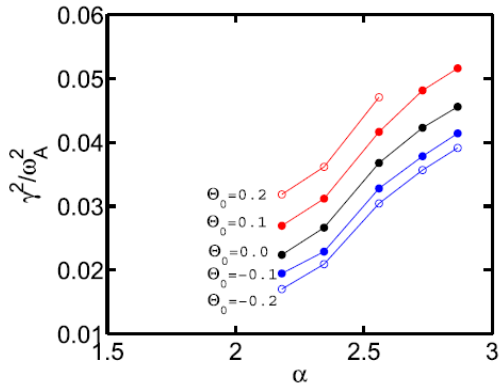

Fig. 4: The relationship between the square of the growth rate and the normalised pressure gradient α for anisotropic plasmas, computed with MISHKA-A with artificial vacuum in the region $\psi_n \geq 0.95$.

Figure 2 shows equilibrium profiles from an illustrative case with $\widetilde{\Theta}_0 = 0.10$. Close inspection of the pressure profiles reveals that $p_\perp$ profile is shifted outboard relative to $p_{||}$. The figure also demonstrates the safety factor for isotropic and anisotropic plasmas agree, $q_a = q_i$, such that the stored thermal energy W_{th} is preserved. Tests were conducted on a series of other anisotropic equilibria with $-0.2 < \widetilde{\Theta}_0 < 0.2$: in all cases the results showed that the *q*, and current profiles, and the thermal energy, were conserved.

The stability of this series of anisotropic equilibrium was analysed using MISHKA-A. Figure 3 shows a plot of the growth rate of the mode against $\widetilde{\Theta}_0$. A clear trend is evident: the growth rate instability increases monotonically with the value of $\widetilde{\Theta}_0$. Over the range $|\widetilde{\Theta}_0| < 0.25$ the growth rate changes by 10%. For the JET and MAST cases discussed, $p_\perp/p_{||} \approx 2.5$ corresponds to $\widetilde{\Theta}_0 = 0.6$, and $p_{||}/p_\perp \approx 1.7$ corresponds to $\widetilde{\Theta}_0 = -0.7$. We thus expect the impact on growth rates for realistic configurations to be significant.

Using MISHKA-A we have also computed the stability with varying normalised pressure gradient α for constant Θ_0. Here, α for an anisotropic plasma is defined by replacing the isotropic pressure according to $p = (2p_\perp + p_{||})/3$. The results are shown in Fig. 4 As α is decreased the growth rate drops, consistent with expectations. Over the parameter range explored the dependence of growth rate with α is unchanged.

4. EQUILIBRIUM REMAPPING FOR ARBITRARY ANISOTROPY

In other work we have also extended the study of anisotropic plasmas to ITER scenario plasmas by developing remapping constraints that first converge HELENA+ATF to arbitrary isotropic static equilibria, add target flow and anisotropy, and then iteratively adjust F^2 to achieve a match with the q profile and hence I_p. The technique also extends Johnston *et al* [11] and the procedure in Sec. 3. The procedure is as follows: the toroidal current can be written

$$J_\phi = -\frac{F(\psi)F'(\psi)}{(1-\Delta)R\mu_0} - \rho\left[T_\parallel{}'(\psi) + H'(\psi) - \left(\frac{\partial W}{\partial \psi}\right)_{\rho,B}\right]. \quad (12)$$

Next, we assume

$$J_{\phi,a} + \frac{F_a(\psi)F_a{}'(\psi)}{(1-\Delta_a)R\mu_0} \approx J_{\phi,i} + \frac{F_i(\psi)F_i{}'(\psi)}{R\mu_0}, \quad (13)$$

and hence

$$J_{\phi,a}(1-\Delta_a)R\mu_0 - J_{\phi,i}R\mu_0 \approx -F_a(\psi)F_a'(\psi) + F_i(\psi)F_i'(\psi), \quad (14)$$

Third, we compute

$$\int_1^{\overline{\psi_n}} \langle J_{\phi,a}(1-\Delta_a)R\mu_0 - J_{\phi,i}R\mu_0\rangle(\psi_a - \psi_0)d\psi_n \approx \left[-{F_a}^2 + {F_i}^2\right] = -\delta F^2(\overline{\psi_n}) + \delta F^2(1), \quad (15)$$

and then update

$$F^2(\overline{\psi_n}) \rightarrow F^2(\overline{\psi_n}) - \delta F^2(\overline{\psi_n}). \quad (16)$$

Finally, we rerun HELENA+ATF and compute

$$\Delta q = \int_0^1 (q_{target} - q)d\psi_n. \quad (17)$$

Equations (15)-(17), and the replacement for F^2, are iterated until $\Delta q < \varepsilon_q$. A second iteration step modifies β until the $\Delta W_{th}/W_{th} < \varepsilon_W$

As an example, Fig. 4 shows the solution across the midplane for a 5MA, B=1.8T (1/3 full field strength) ITER scenario. Both isotropic (red) and anisotropic (blue) equilibrium solutions are shown, with the later for $T_\parallel/T_\perp = 0.8$. The solution has been iterated until $\varepsilon_q = \varepsilon_W = 0.01$.

As an initial illustration of the technique, we have projected ITER solutions for $T_\parallel/T_\perp = 0.8$ and $T_\parallel/T_\perp = 1.2$, shown in Fig. 6. This shows the displacement of the p|| surfaces outboard / inboard from flux surfaces respectively, in agreement with previous trends identified by Cooper et al.[12]

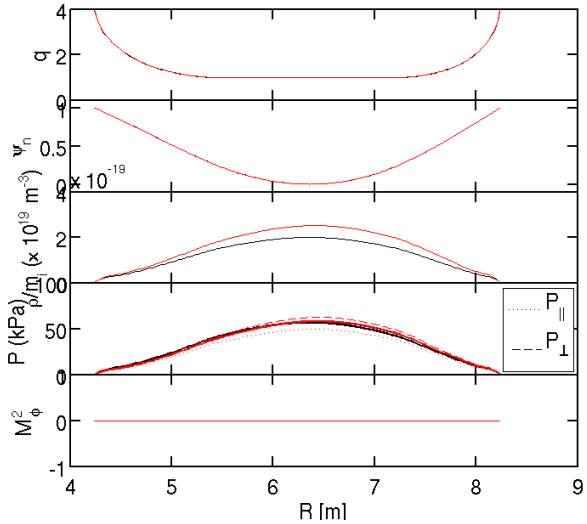

Fig. 5: 5MA, B=1.8T (1/3 field) ITER scenario across the midplane for both isotropic (red) and anisotropic (blue) solutions using the remapping of Eqs. (15)-(17). The panel shows q profile, poloidal flux, number density, pressure and toroidal Mach number.

Finally, Fig. 7 shows the dependence of peak mass density and magnetic axis as a function of core anisotropy parameter $\widetilde{\Theta}_0$. An increasing outboard shift is evident for $\widetilde{\Theta}_0 > 0$ ($T_\parallel > T_\perp$), while for $\widetilde{\Theta}_0 < 0$ ($T_\parallel < T_\perp$) the shift is inboard. The increase in on-axis mass density occurs because the Bernoulli function H(ψ) has not been normalised account for a change in $\widetilde{\Theta}_0$.

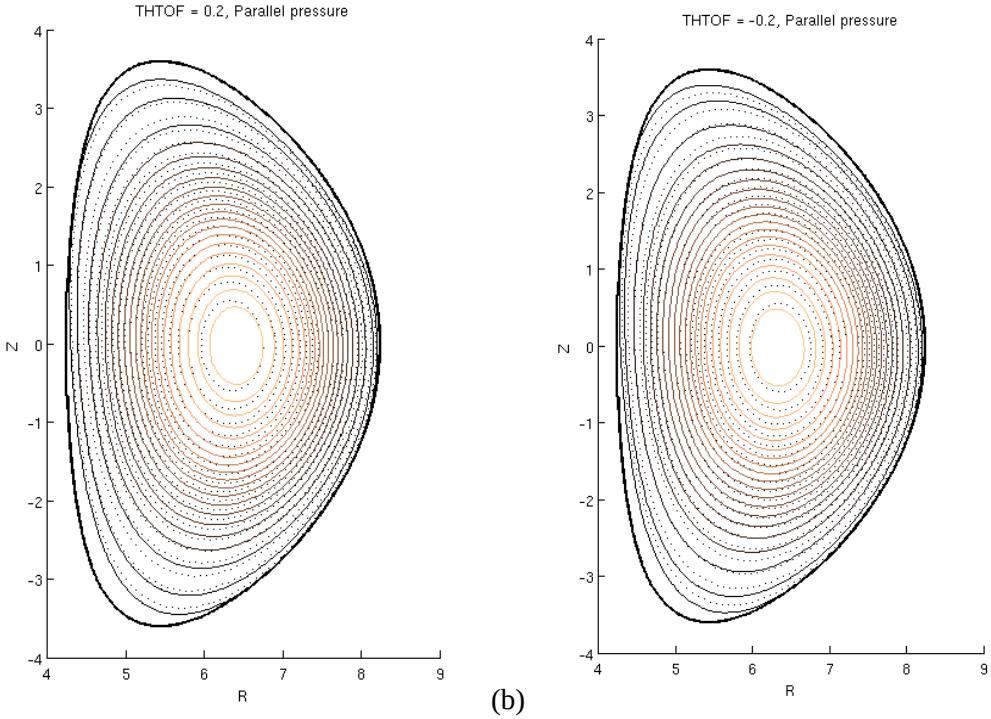

(a) (b)

Fig. 6: Parallel pressure surfaces displaced outboard / inboard from flux surfaces respectively, for $T_\parallel/T_\perp = 0.8$ (Θ_0=0.2) and $T_\parallel/T_\perp = 1.2$ (Θ_0=-0.2).

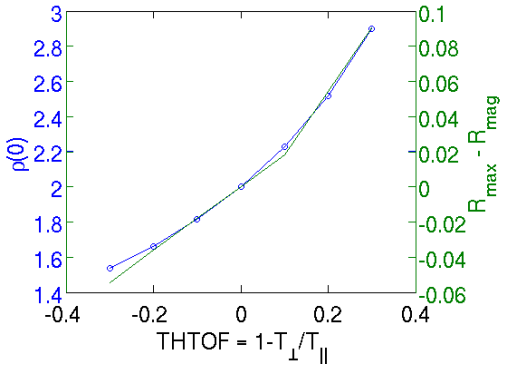

Fig. 7: Variation of density and pressure from magnetic axis with anisotropy parameter $\widetilde{\Theta}_0 = T_0/T_{||}\left(1 - T_{||}/T_\perp\right)$.

5. CONCLUSIONS

In this work we have examined the impact of pressure anisotropy on ballooning mode stability. This was accomplished by inclusion of anisotropy in the equilibrium, enabling the calculation of linear stability and growth rates in realistic configurations. The work presented here is a scoping study applied in a cylindrical cross-section large aspect ratio tokamak plasma, and we have studied the stability of an n=30 ELM as the level of anisotropy changes. The primary result is that the growth rate increases with increasing core anisotropy parameter Θ_0. As $T_\perp$ increases over $T_{||}$, $p_\perp$ surfaces are displaced outboard toward the bad curvature region, and the mode becomes more unstable. Conversely, an inward shift of surfaces acts to stabilise the mode. This is consistent with the literature (see Salberta et al [13]).

Over the range $|\Theta_0| < 0.20$, which corresponds to the range $0.69 < p_{||}/p_\perp < 1.34$ at the outboard location where the eigenmode is peak, the growth rate changes by 10%. Experimentally, values of $p_\perp/p_{||} > 2.5$ (corresponding to $\Theta_0 = 0.6$), and $p_{||}/p_\perp > 1.7$ (corresponding to $\Theta_0 = -0.7$) have been identified in JET and MAST plasmas, respectively. This suggests that the impact on growth rates may be significant, and indeed offer the possibility that higher ELM-free performance might be achieved by increasing $p_\parallel/p_\perp$ in the pedestal region.

We are in the process of adding a vacuum region to the code MISHKA-A, and plan to examine the effect of anisotropy on a broader spectrum of peeling-ballooning modes. The analysis will also be repeated using non-circular boundaries and arbitrary cross-section for the plasma.

In other work we have also commenced a study of the impact of anisotropy on ITER scenarios, and have further extended the equilibrium remapping technique to enable a more complete study of equilibrium and stability in arbitrary cross-section. We have computed the displacement of pressure surfaces from flux surfaces for prescribed levels of anisotropy, and demonstrated that the trends are consistent with the literature. In ongoing work we are constructing the anisotropy in the plasma profile from ICRH heating studies, as well as computing the change to the continuum and mode structures for expected levels of anisotropy in ITER.

ACKNOWLEDGEMENTS

The authors wish to thank S. Pinches and SM. Schneider of the ITER Organization and O. Sauter of the Swiss Plasma Center. We also wish to acknowledge funding support through the Australian Research Council DP140100790, the Mathematical Sciences Institute of the Australian National University, and the Australian Nuclear and Science Technology Organisation.

REFERENCES

[1] M. J. HOLE, M. FITZGERALD, Plasma Phys. Control. Fusion **56** (2014) 053001

[2] W. ZWINGMANN, L. G. ERIKSSON, P. STUBBERFIELD. Plasma Phys. Control. Fusion, 43(11):1441, 2001.

[3] M. J. HOLE *et al* Plasma Phys. Con. Fus., 53(7):074021, 2011.

[4] Z. S. QU, M. FITZGERALD, M..HOLE. Plasma Phys. Control. Fusion, 56(7):075007, 2014.

[5] Z. S. QU, M J HOLE, M. FITZGERALD, Plasma Phys. Control. Fusion 57 (2015) 095005

[6] 0. P. POGUTSE, N. V. CHUDIN, E. I. YURCHENKO. Sov. J. Plasma Phys., 9(1):96–100, 1983

[7] J. P. GOEDBLOED, S. POEDTS. *Advanced magnetohydrodynamics: with applications to laboratory and astrophysical plasmas*. Cambridge university press, 2010

[8] M. SCHNEIDER *et al* 144th EPS Conference on Plasma Physics, P5.153, 26-30 June 2017

[9] A. B. MIKHAILOVSKII, G. T. A. HUYSMANS, W. O. K. KERNER, S. E. SHARAPOV 1997 Optimization of computational MHD normal-mode analysis for tokamaks Plasma Phys. Rep. 23 844–57

[10] G. T. A. HUYSMANS, S.E. SHARAPOV, A. B. MIKHAILOVSKII, W. KERNER. Physics of Plasmas, 8(10):4292–4305, 2001

[11] A. JOHNSTON, M. J. HOLE, Z. S. QU, H. HEZAVEH, Plasma Phys. Control. Fusion 60 (2018) 065006

[12] W.A. Cooper *et al* 1980 *Nucl. Fusion* **20** 985

[13] E. R. SALBERTA, R. C. GRIMM, J. L. JOHNSON, J. MANICKAM, W. M. TANG 1987 Anisotropic pressure tokamak equilibrium and stability considerations Phys. Fluids 30 2796